

# Integrated Autopilot Tuning and Unmanned Aerial Vehicle Design

*Assist. Prof. Dr. Tugrul OKTAY\**, *PhD Candidate Mehmet KONAR\*\**, *Assist. Prof. Dr. Murat ONAY\*\*\**, and *MS Candidate Mohamed Abdallah Mohamed\*\*\*\**

*\*, \*\*, \*\*\*, \*\*\*\* Erciyes University*

*College of Aviation, Melikgazi, Kayseri, TURKEY, 38039*

## Abstract

In this conference paper it is aimed to increase autonomous flight performance of a small unmanned aerial vehicle (UAV) through integrated autopilot system parameters (i.e. P, I, D gains) and UAV parameters (i.e. assembly points of wing and tailplane to fuselage) design. For this purpose a small UAV (i.e. ZANKA-I) is manufactured in Erciyes University, College of Aviation, Model Aircraft Laboratory is used. Optimum values of UAV parameters and autopilot parameters are determined using a stochastic optimization method. Using this approach autonomous flight performance of UAV is considerably improved. Integrated design approach satisfies confidence, high performance and easy-utility request of UAV users.

## 1. Introduction

For the around last four and five decades Unmanned Air Vehicles (UAVs) have been broadly used for both military operations and also in commercial applications since they have many superiorities with respect to the manned vehicles. Some of these superiorities are having lower cost in manufacturing and operating, having simplicity in configuration depending on customer demand and also they do not risk the pilot's life on problematic missions. UAVs have been used in aerial photography (e.g. film and video), agriculture (i.e. crop monitoring and spraying), customs and excise, electricity companies, coast guarding, conservation, fire services and forestry, fisheries, gas and oil supply companies etc. with civilian purposes. They have also been benefited during military tasks. For instance, they have been applied for navy (e.g. shadowing enemy fleets), army (e.g. reconnaissance) and air force (e.g. radar system jamming and destruction). For more UAV applications, Austin R., 2010 [1] can be visited. Many scientific studies on UAV design and control have been also followed recently (e.g. Ding, Liu and Hsiao; 2013 [2]; Drak et al. 2014 [3]; Filippis, Guglieri, Quagliotti, 2014 [4]; Hadi et al. 2014 [5]).

In conventional method, a model of the any physical system will be controlled (e.g. fixed wing UAV, hybrid UAV, helicopter UAV, any structure, etc.), also called as the "plant", is given a priori to the control engineer who has no influence on this physical system's design. Nonetheless, it is well-known reality that the plant design problem and control system design problem are not irrelevant (see Grigoriadis et al., 1993 [6]; Grigoriadis et al., 1996 [7]). Some minor changes in UAV parameters may improve autonomous performance significantly as examined, for instance, in Krog et al., 2004 [8]; Park et al., 2008 [9]; Qun and Hong-quang, 2011 [10]. The traditional chronological methodology: firstly, design the plant, and secondly design the controller, does not distribute the best complete design (see Grigoriadis et al., 1993 [6]; Grigoriadis et al., 1996 [7]). Elegantly, the system to be controlled and the controller should be simultaneously designed so that a given objective (i.e. cost function) is minimized, while there are constraints on the system and control system parameters. In this conference article this idea is pursued and a small UAV (i.e. ZANKA-I) manufactured in Erciyes University, College of Aviation and PID based hierarchical autopilot system are simultaneously designed through wing-fuselage and tail-fuselage assembly parameters and also autopilot P, I, D parameters for minimizing a cost function consisting of performance parameters, i.e. maximum overshoot, settling time and rise time during trajectory tracking.

Autopilots are such systems that guide UAVs for the duration of flight without any assistance of human workers. Autopilots is an onboard intelligent system and they consist of state sensors and controllers. State sensors continuously measure several parameters of UAV using various sensors, e.g. GPS, accelerometer, magnetometer, gyros, pitot-tube. Controllers use these measurements and calculate the error between current and required states.

The control signal is influenced by the error signal and it is produced to actuate the several control surfaces of the aircraft UAV. Due to fact that aircraft dynamics is exceedingly nonlinear, many intelligent control techniques, e.g., PID control, neural network, fuzzy logic, sliding mode control, etc., have been used for autopilots for promising a smooth appropriate trajectory navigation (see Chao et al., 2007 [11] for more discussion). In this conference article, an autopilot system having PID based hierarchical control structure is benefited. Recently, PID based control systems have been used by different scientists successfully (e.g. see Jung et al., 2009 [12]; Sartori, 2014[13]).

This is the *first conference article* simultaneously designing a small UAV and autopilot system for autonomous performance maximization. Furthermore, for this purpose a stochastic optimization method (i.e. SPSA, simultaneous perturbation stochastic approximation) is *first time* applied and using it, optimal results are found fast and safely. Moreover, simultaneous design idea progresses autonomous flight performance noticeably, therefore less overshoot, less settling time and less rise time are obtained during trajectory tracking.

## 2. Dynamic Modeling of UAV (i.e. Zanka-I)

Longitudinal and lateral linearized state-space models of a fixed-wing aircraft are given in Eqs. (1) and (2), respectively (see Ref. [14] for more details)

$$\begin{bmatrix} \dot{x}_l \\ \Delta \dot{u} \\ \Delta \dot{w} \\ \Delta \dot{q} \\ \Delta \dot{\theta} \\ \Delta \dot{h} \end{bmatrix} = \underbrace{\begin{bmatrix} X_u & X_w & 0 & -g & 0 \\ Z_u & Z_w & u_0 & 0 & 0 \\ M_u + M_w Z_w & M_w + M_w Z_w & M_q + M_w u_0 & 0 & 0 \\ 0 & 0 & 1 & 0 & 0 \\ -\sin(\theta_0) & \cos(\theta_0) & 0 & -u_0 \cos(\theta_0) & 0 \end{bmatrix}}_{A_l} \begin{bmatrix} x_l \\ \Delta u \\ \Delta w \\ \Delta q \\ \Delta \theta \\ \Delta h \end{bmatrix} + \underbrace{\begin{bmatrix} X_{\delta_T} & X_{\delta_e} \\ Z_{\delta_T} & Z_{\delta_e} \\ M_{\delta_T} + M_w Z_{\delta_T} & M_{\delta_e} + M_w Z_{\delta_e} \\ 0 & 0 \\ 0 & 0 \end{bmatrix}}_{B_l} \begin{bmatrix} u_l \\ \Delta \delta_T \\ \Delta \delta_e \end{bmatrix} \quad (1)$$

$$\begin{bmatrix} \dot{x}_{la} \\ \Delta \dot{\beta} \\ \Delta \dot{p} \\ \Delta \dot{r} \\ \Delta \dot{\phi} \\ \Delta \dot{\psi} \end{bmatrix} = \underbrace{\begin{bmatrix} \frac{Y_\beta}{u_0} & \frac{Y_p}{u_0} & -(1 - \frac{Y_r}{u_0}) & -\frac{g}{u_0} \cos(\theta_0) & 0 \\ L_\beta^* + \frac{I_{xz}}{I_{xx}} N_\beta^* & L_p^* + \frac{I_{xz}}{I_{xx}} N_p^* & L_r^* + \frac{I_{xz}}{I_{xx}} N_r^* & 0 & 0 \\ N_v^* + \frac{I_{xz}}{I_{zz}} L_v^* & N_p^* + \frac{I_{xz}}{I_{zz}} L_p^* & N_r^* + \frac{I_{xz}}{I_{zz}} L_r^* & 0 & 0 \\ 0 & 1 & 0 & 0 & 0 \\ 0 & 0 & \sec(\theta_0) & 0 & 0 \end{bmatrix}}_{A_{la}} \begin{bmatrix} x_{la} \\ \Delta \beta \\ \Delta p \\ \Delta r \\ \Delta \phi \\ \Delta \psi \end{bmatrix} + \underbrace{\begin{bmatrix} 0 & \frac{Y_{\delta_r}}{u_0} \\ L_{\delta_a}^* + \frac{I_{xz}}{I_{xx}} N_{\delta_a}^* & L_{\delta_r}^* + \frac{I_{xz}}{I_{xx}} N_{\delta_r}^* \\ N_{\delta_a}^* + \frac{I_{xz}}{I_{zz}} L_{\delta_a}^* & N_{\delta_r}^* + \frac{I_{xz}}{I_{zz}} L_{\delta_r}^* \\ 0 & 0 \\ 0 & 0 \end{bmatrix}}_{B_{la}} \begin{bmatrix} u_{la} \\ \Delta \delta_a \\ \Delta \delta_r \end{bmatrix} \quad (2)$$

For 60 km/h straight level flight condition numerical state space models are:

$$\begin{bmatrix} \dot{x}_l \\ \Delta \dot{u} \\ \Delta \dot{w} \\ \Delta \dot{q} \\ \Delta \dot{\theta} \\ \Delta \dot{h} \end{bmatrix} = \underbrace{\begin{bmatrix} -6.5179e-2 & 8.3424e-1 & 0 & -9.81 & 0 \\ -1.9744 & -7.3459 & 1.6667e+1 & 0 & 0 \\ 3.2691e-1 & -1.0848 & -7.4293 & 0 & 0 \\ 0 & 0 & 1 & 0 & 0 \\ -5.2336e-2 & 9.9863e-1 & 0 & -16.6438 & 0 \end{bmatrix}}_{A_l} \begin{bmatrix} x_l \\ \Delta u \\ \Delta w \\ \Delta q \\ \Delta \theta \\ \Delta h \end{bmatrix} + \underbrace{\begin{bmatrix} 6.9709 & 0 \\ 0 & -8.0041 \\ 1.4268 & -6.0562e+1 \\ 0 & 0 \\ 0 & 0 \end{bmatrix}}_{B_l} \begin{bmatrix} u_l \\ \Delta \delta_T \\ \Delta \delta_e \end{bmatrix} \quad (3)$$

$$\begin{matrix} \dot{x}_{la} \\ \Delta\dot{\beta} \\ \Delta\dot{p} \\ \Delta\dot{r} \\ \Delta\dot{\phi} \\ \Delta\dot{\psi} \end{matrix} = \begin{matrix} A_{la} \\ \begin{bmatrix} -4.1954e-3 & 0 & -9.9985e-1 & 5.8824e-1 & 0 \\ 2.3668e-2 & -2.3285e+1 & 4.6459 & 0 & 0 \\ 1.8318e-1 & -3.5980 & 2.2331e-1 & 0 & 0 \\ 0 & 1 & 0 & 0 & 0 \\ 0 & 0 & 1.0014 & 0 & 0 \end{bmatrix} \end{matrix} \begin{matrix} x_{la} \\ \Delta\beta \\ \Delta p \\ \Delta r \\ \Delta\phi \\ \Delta\psi \end{matrix} + \begin{matrix} B_{la} \\ \begin{bmatrix} 0 & 2.0062e-3 \\ 3.4630e+2 & 1.2164e+1 \\ -9.8826 & 4.7664e-1 \\ 0 & 0 \\ 0 & 0 \end{bmatrix} \end{matrix} \begin{matrix} u_{la} \\ \Delta\delta_a \\ \Delta\delta_r \end{matrix} \quad (4)$$

The flight dynamics modes of UAV (i.e. ZANKA-I) are given in Fig. 1. From these figure it can be easily seen that qualitative and quantitative behaviors of flight dynamics modes are similar with the ones given in Zagi web site [15]; Yenil and Hajiyeve (2008 and 2013) [16-17]; Cardenas (2012) [18]; Jeni and Budiyono (2006) [19].

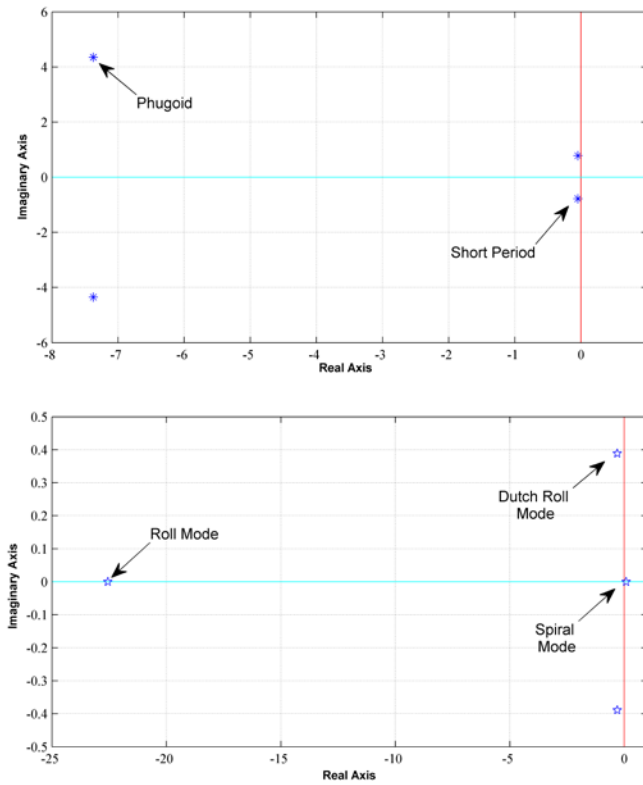


Figure 1: Longitudinal and Lateral Flight Dynamics Modes



Figure 2: Photos of ZANKA-I and Its Passive Morphing Equipment

In Fig. 2 some photos of ZANKA-I UAV and its pasisve morphing equipments are given. When gust disturbance exists, the parametrical state-space models are

$$\begin{bmatrix} \dot{x}_i \\ \Delta \dot{u} \\ \Delta \dot{w} \\ \Delta \dot{q} \\ \Delta \dot{\theta} \end{bmatrix} = \underbrace{\begin{bmatrix} X_u & X_w & 0 & -g \\ Z_u & Z_w & u_0 & 0 \\ M_u + M_w Z_w & M_w + M_w Z_w & M_q + M_w u_0 & 0 \\ 0 & 0 & 1 & 0 \end{bmatrix}}_{A_i} \begin{bmatrix} x_i \\ \Delta u \\ \Delta w \\ \Delta q \\ \Delta \theta \end{bmatrix} + \underbrace{\begin{bmatrix} X_{\delta_T} & X_{\delta_e} \\ Z_{\delta_T} & Z_{\delta_e} \\ M_{\delta_T} + M_w Z_{\delta_T} & M_{\delta_e} + M_w Z_{\delta_e} \\ 0 & 0 \end{bmatrix}}_{B_i} \begin{bmatrix} u_i \\ \Delta \delta_T \\ \Delta \delta_e \end{bmatrix} + \underbrace{\begin{bmatrix} -X_u & -X_w & 0 \\ -Z_u & -Z_w & 0 \\ -M_u & -M_w & -M_q \\ 0 & 0 & 0 \end{bmatrix}}_{B_{i,gust}} \begin{bmatrix} u_{i,gust} \\ w_g \\ q_g \end{bmatrix} \quad (5)$$

$$\begin{bmatrix} \dot{x}_{ia} \\ \Delta \dot{\beta} \\ \Delta \dot{p} \\ \Delta \dot{r} \\ \Delta \dot{\phi} \end{bmatrix} = \underbrace{\begin{bmatrix} \frac{Y_\beta}{u_0} & \frac{Y_p}{u_0} & -(1-\frac{Y_r}{u_0}) & -\frac{g}{u_0} \cos(\theta_0) \\ \frac{L_\beta^* + \frac{I_{xz}^*}{I_{xx}^*} N_\beta^*}{L_\beta^* + \frac{I_{xz}^*}{I_{xx}^*} N_\beta^*} & \frac{L_p^* + \frac{I_{xz}^*}{I_{xx}^*} N_p^*}{L_p^* + \frac{I_{xz}^*}{I_{xx}^*} N_p^*} & \frac{L_r^* + \frac{I_{xz}^*}{I_{xx}^*} N_r^*}{L_r^* + \frac{I_{xz}^*}{I_{xx}^*} N_r^*} & 0 \\ N_\beta^* + \frac{I_{xz}^*}{I_{zz}^*} L_\beta^* & N_p^* + \frac{I_{xz}^*}{I_{zz}^*} L_p^* & N_r^* + \frac{I_{xz}^*}{I_{zz}^*} L_r^* & 0 \\ 0 & 1 & 0 & 0 \end{bmatrix}}_{A_{ia}} \begin{bmatrix} x_{ia} \\ \Delta \beta \\ \Delta p \\ \Delta r \\ \Delta \phi \end{bmatrix} + \underbrace{\begin{bmatrix} 0 & \frac{Y_{\delta_r}}{u_0} \\ L_{\delta_a}^* + \frac{I_{xz}^*}{I_{xx}^*} N_{\delta_a}^* & L_{\delta_r}^* + \frac{I_{xz}^*}{I_{xx}^*} N_{\delta_r}^* \\ N_{\delta_a}^* + \frac{I_{xz}^*}{I_{zz}^*} L_{\delta_a}^* & N_{\delta_r}^* + \frac{I_{xz}^*}{I_{zz}^*} L_{\delta_r}^* \\ 0 & 0 \end{bmatrix}}_{B_{ia}} \begin{bmatrix} u_{ia} \\ \Delta \delta_a \\ \Delta \delta_r \end{bmatrix} + \underbrace{\begin{bmatrix} \frac{Y_\beta}{u_0} & 0 & 0 \\ -L_\beta^* \frac{I_{xz}^*}{I_{xx}^*} N_\beta^* & -L_p^* \frac{I_{xz}^*}{I_{xx}^*} N_p^* & -L_r^* \frac{I_{xz}^*}{I_{xx}^*} N_r^* \\ -N_\beta^* \frac{I_{xz}^*}{I_{zz}^*} L_\beta^* & -N_p^* \frac{I_{xz}^*}{I_{zz}^*} L_p^* & -N_r^* \frac{I_{xz}^*}{I_{zz}^*} L_r^* \\ 0 & 0 & 0 \end{bmatrix}}_{B_{ia,gust}} \begin{bmatrix} u_{ia,gust} \\ v_g / u_0 \\ p_g \\ r_g \end{bmatrix} \quad (6)$$

For this article Von-Karman Turbulence modeling approach is applied (U.S. Military Handbook MIL-HDBK-1797, 1997 [20]).

### 3. Autopilot system

For our both theoretical and practical (with real-time flight tests) studies traditional PID based hierarchical autopilot system is applied (see Refs. [11,21]). It has three layers PID controller to succeed waypoint navigation (see Fig. 3).

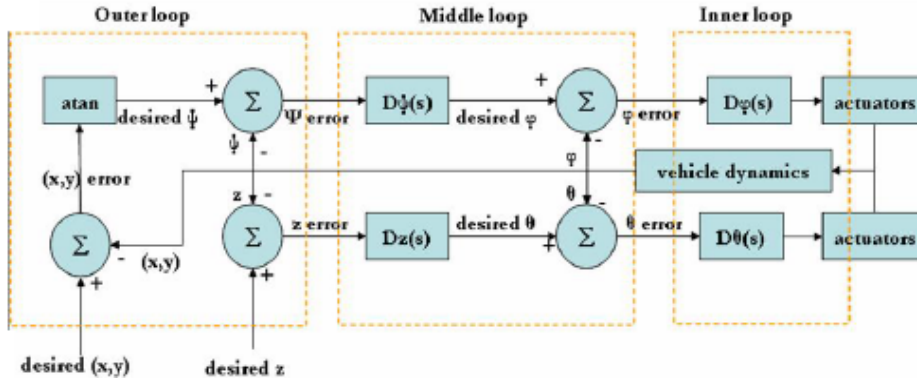


Figure 3: Classical Hierarchical Autopilot System Structure (taken from Ref. [11])

### 4. Problem Formulation and Optimization Technique

In most general situation PID based hierarchical autopilot system structure lets height, yaw angle, and velocity trajectory tracking. This systems have 6 P-I-D controllers in 3 layers (i.e. outer layer, middle layer and inner layer). These PIDs have upper and lower bounds and satisfy trajectory tracking. If any interested autopilot user demands to use all of them, it is required to tune 18 parameters (i.e. 6 P parameters, 6 I parameters and 6 D parameters). However, in this article for simultaneous UAV tuning and control system (i.e. autopilot) design idea there are two additional structural parameters (optimum assembly points of wing and horizontal tail to fuselage). A cost function

consisting of settling time, rise time and overshoot is useful choice for high-performance trajectory tracking (see Eq. (7)).

$$\mathbf{J} = \sum g(T_{st} - T_{st_u})^2 + g(T_{rt} - T_{rt_u})^2 + g(\%OS - \%OS_u)^2 \quad (7)$$

The simultaneous optimization problem can be expressed as follows:

$\min\{\mathbf{J}\}$  where

$$\mathbf{J} = f\left(x_{w\_play}, x_{ht\_play}, K_{P_1}, K_{I_1}, K_{D_1}, K_{P_2}, K_{I_2}, K_{D_2}, \dots, K_{P_6}, K_{I_6}, K_{D_6}\right) \quad (8)$$

and it is function of 20 terms (2 UAV structural parameters and 18 autopilot system design parameters). Terms of cost function is calculated in this article as follows:

$$\text{If } T_{st} \leq T_{st_u}, g(T_{st} - T_{st_u})^2 = 0 \text{ else}$$

$$T_{st} \leq T_{st_u}, g(T_{st} - T_{st_u})^2 = (T_{st} - T_{st_u})^2 \quad (9a)$$

$$\text{If } T_{rt} \leq T_{rt_u}, g(T_{rt} - T_{rt_u})^2 = 0 \text{ else } T_{rt} \leq T_{rt_u}, g(T_{rt} - T_{rt_u})^2 = (T_{rt} - T_{rt_u})^2 \quad (9b)$$

$$\text{If } \%OS \leq \%OS_u, g(\%OS_{rr} - \%OS_{rt_u})^2 = 0 \text{ else } \%OS \leq \%OS_u, g(\%OS - \%OS_u)^2 = 0 \quad (9c)$$

### Simultaneous Perturbation Stochastic Approximation (SPSA)

Because of the fact that there is complex dependency between  $\mathbf{J}$  (see Eq. (7)) and the constraints on the optimization variables (18 P-I-D gains and 2 UAV structural parameters, total of 20 parameters), computation of cost function derivatives with respect to these parameters is not analytically possible. This advocates the demand of certain stochastic optimization techniques. In order to solve this complex problem for this conference article we select a stochastic optimization method called as SPSA, which was successfully used in similar complex constrained optimization problems previously (see Sultan, 2010 [22]; Oktay 2012 [23]; Oktay and Sultan 2012 [24]). SPSA has many superiorities w.r.t. the other existing method in the literature. First of all, SPSA is inexpensive because it uses only two evaluations of the objective to estimate the gradient (see Spall 1992). Furthermore, it is also successful in solving constrained optimization problems (see Sultan, 2010 [22]; Oktay 2012 [23]; Oktay and Sultan 2013 [24]). Its brief description is given next.

Let  $\Psi$  denote the vector of optimization variables. For the classical SPSA, if  $\Psi_{[k]}$  is the estimate of  $\Psi$  at k-th iteration, then  $\Psi_{[k+1]} = \Psi_{[k]} - \Psi_k g_{[k]}$ , where

$$g_{[k]} = \left[ \frac{\Gamma_+ - \Gamma_-}{2d_k \Delta_{[k]1}} \dots \frac{\Gamma_+ - \Gamma_-}{2d_k \Delta_{[k]p}} \right]^T \quad (10)$$

$a_k$  and  $d_k$  are gain sequences,  $g_{[k]}$  is the estimate of the objective's gradient at  $\Psi_{[k]}$ ,  $\Delta_{[k]} \in R^p$  is a vector of p mutually independent mean-zero random variables  $\{\Delta_{[k]1} \dots \Delta_{[k]p}\}$  satisfying definite requirements (see Sadegh and Spall, 1998 [25]; He et al., 2003 [26]),  $\Gamma_+$  and  $\Gamma_-$  are estimates of the objective evaluated at  $\Psi_{[k]} + d_k \Delta_{[k]}$  and

$\Psi_{[k]} - d_k \Delta_{[k]}$ , respectively. The adaptation is through using gain sequences  $a_k$  and  $d_k$ , which is required to change according to

$$a_k = \min \left\{ a / (S+k)^\lambda, 0.95 \min_i \{ \min(\mu_{l_i}), \min(\mu_{u_i}) \} \right\} \quad (11a)$$

$$d_k = \min \left\{ d / k^\Theta, 0.95 \min_i \{ \min(\eta_{l_i}), \min(\eta_{u_i}) \} \right\} \quad (11b)$$

where  $\eta_{l_i}$  and  $\eta_{u_i}$  are vectors whose components are  $(\Psi_{[k]i} - \Psi_{min_i}) / \Delta_{[k]i}$  for each positive  $\Delta_{[k]i}$  and  $(\Psi_{max_i} - \Psi_{[k]i}) / \Delta_{[k]i}$  for each negative  $\Delta_{[k]i}$ , respectively. Similarly,  $\mu_{l_i}$  and  $\mu_{u_i}$  are vectors whose components are  $(\Psi_{[k]i} - \Psi_{min_i}) / g_{[k]i}$  for each positive  $g_{[k]i}$  and  $(\Psi_{[k]i} - \Psi_{max_i}) / g_{[k]i}$  for each negative  $g_{[k]i}$ , respectively and  $d, a, \lambda, \Theta, S$  are other SPSA parameters.

### Algorithm of SPSA For Simultaneous UAV Design and Autopilot System Tuning

Step 1: Set  $k=1$  and choose initial values for the optimization parameters,  $\Psi = \Psi_{[k]}$ , and a specific flight condition (e.g. straight level flight at speed  $V_A = 60$  km/h).

Step 2: Compute  $A_p$  and  $B_p$ , design the corresponding autopilot system and obtain the current value of the objective,  $\Gamma_k$  given by Equation (7) (note that  $\Gamma_k = J_k$  for our autopilot system).

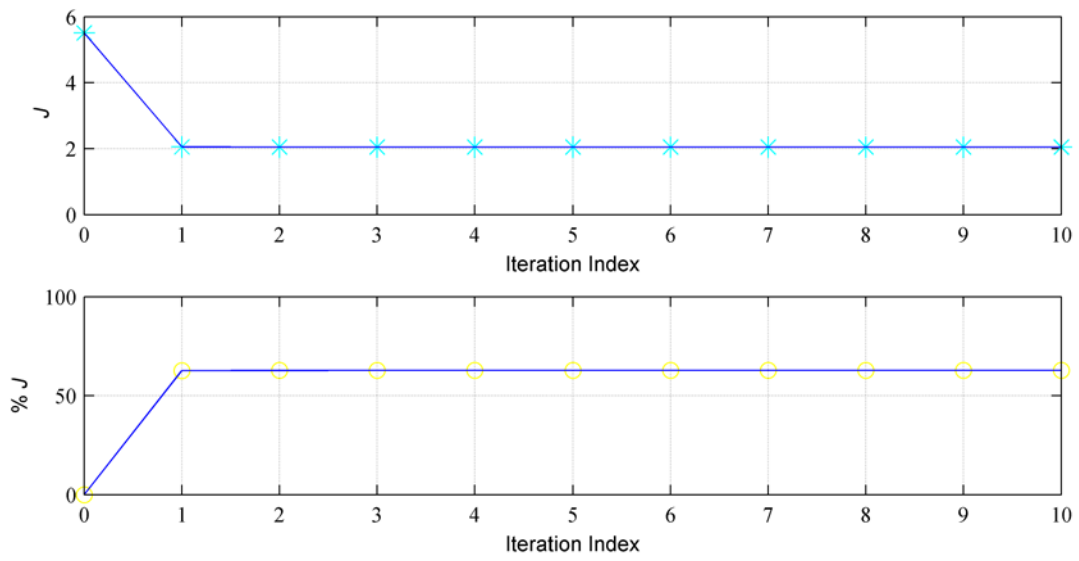
Step 3: Perturb  $\Psi_{[k]}$  to  $\Psi_{[k]} + d_k \Delta_{[k]}$  and  $\Psi_{[k]} - d_k \Delta_{[k]}$  and solve the corresponding autopilot system in order to obtain  $\Gamma_+$  and  $\Gamma_-$ , respectively. Then compute the approximate gradient,  $g_{[k]}$ , using Eq. (10) with  $d_k$  given by Eq. (11b).

Step 4: If  $\|a_k g_{[k]}\| < \delta \Psi$ , where  $a_k$  is given by Eq. (9a) and  $\delta \Psi$  is the minimum allowed variation of  $\Psi$ , or  $k+1$  is greater than the maximum number of iterations allowed, exit, else calculate the next estimate of  $\Psi$ ,  $\Psi_{[k+1]}$ , using  $\Psi_{[k+1]} = \Psi_{[k]} - a_k g_{[k]}$ , set  $k=k+1$  and return to Step 2.

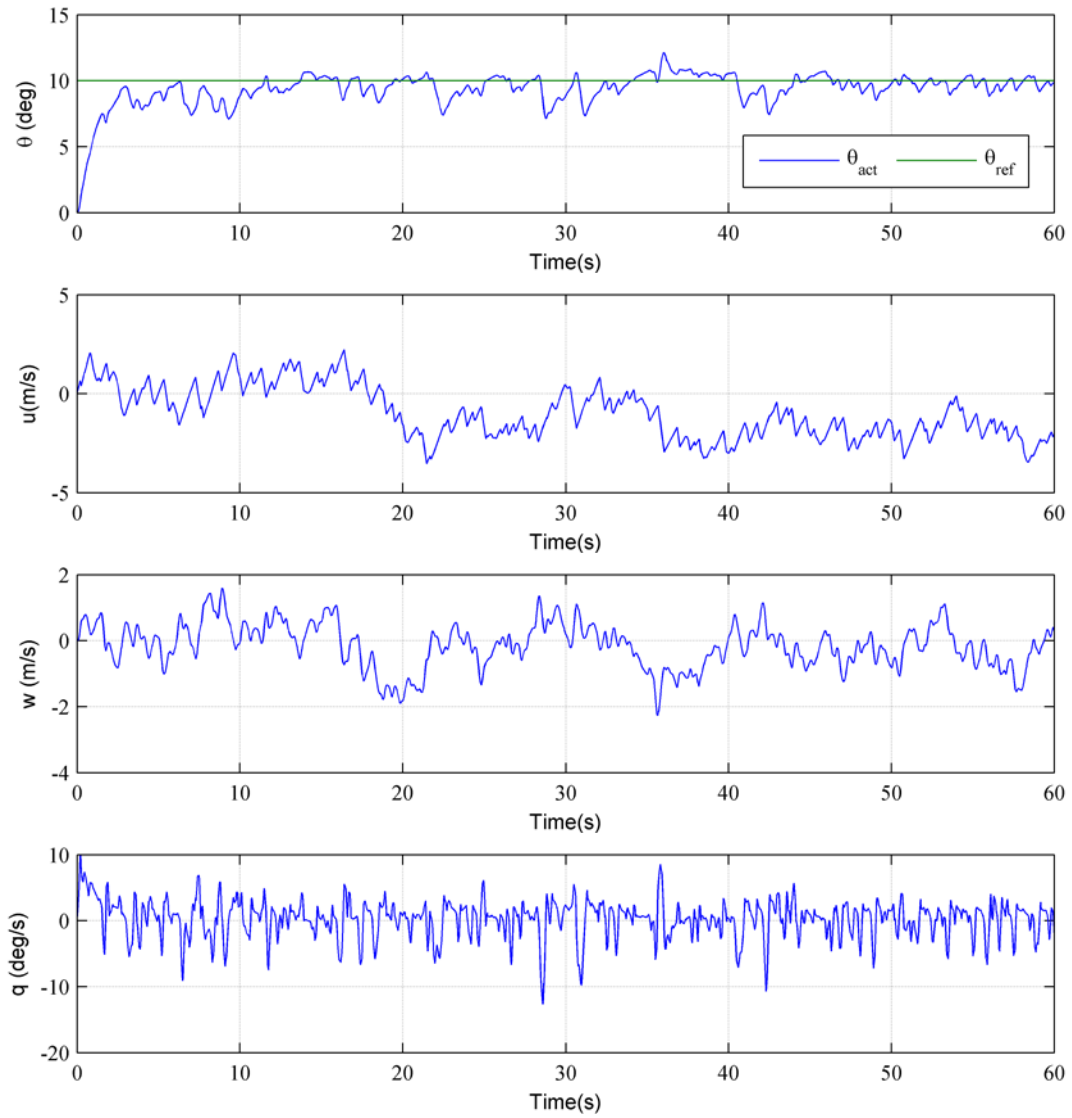
## 5. Simultaneous Morphing UAV and Autopilot System Design Results

Small UAV (i.e. ZANKA-I) and autopilot system (for pitch attitude tracking) are simultaneously designed for minimizing cost function (see Eq. 7) using SPSA. For this conference article the ZANKA-I UAV was tracking a 10 degrees of pitch angle and there were a PID controller parameters and two structural parameters (i.e. assembly points of wing and tailplane to fuselage) during this optimization problem. SPSA parameters applied were:  $S=5$ ,  $a=100$ ,  $\lambda=0.602$ ,  $d=20$ ,  $\Theta=0.101$ . After 10 iterations optimum parameters found were:  $x_{w\_play} = 44.9287$ ,  $x_{t\_play} = 15.0002$  mm,  $K_{P_\theta} = 74.9999$ ,  $K_{I_\theta} = 2.5070$ ,  $K_{D_\theta} = 74.9999$ . In Fig. 4 response of ZANKA-I for desired pitch angle, cost minimization during using SPSA, and relative energy save at each iteration are given. The relative energy save  $\%J$  is:  $\%J = 100(J_0 - J_f) / J_0$  where  $J_0$  and  $J_f$  are costs of performance for initial and final situations, respectively.

From Fig. 4 and 5 it can be expressed that autopilot system is very successful during tracking reference trajectory. Furthermore, SPSA is very fast and effective during energy minimization. In final, considerable energy (around %62.8) is saved using simultaneous small UAV design and autopilot system tuning.



**Fig. 4** SPSA Application and Relative Energy Save



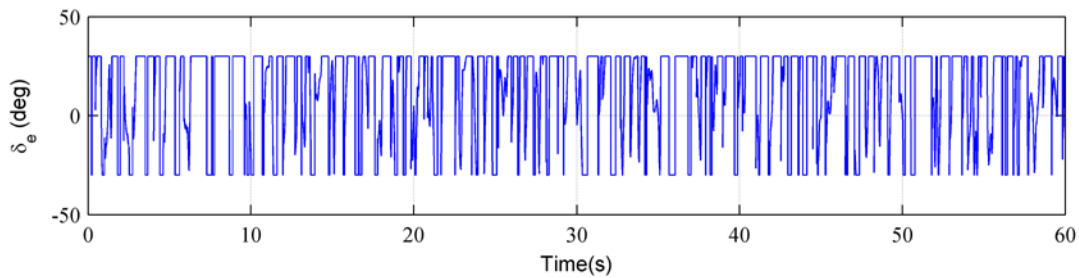


**Fig. 5** Simulation Results

## 6. Conclusions

Simultaneous small unmanned aerial vehicle (UAV) design and autopilot system tuning is investigated in order to advance autonomous flight performance of small UAVs. Dynamic modeling of a fixed-wing aircraft is shortly expressed. Obtained models are validated using existing data in the UAV literature. A PID based hierarchical autopilot system is benefited for this conference study. A stochastic optimization method namely simultaneous perturbation and stochastic approximation (i.e. SPSA) is used for autonomous performance maximization. Important improvement in flight performance (around %62.8) is found using simultaneous small UAV design and autopilot system tuning idea. This satisfied the general UAV requirements of less overshoot, less settling and less rise time s. Closed-loop responses when there is pure turbulence during flight is also examined and satisfactory results (meaning that small rise and settling time and small overshoot) are found. This conference article study satisfies UAV users confidence, high performance, and easy utility.

## Acknowledgement

This work was supported by Research Fund of The Scientific and Technological Research Council of Turkey (TÜBİTAK) under Project Number: 114M856.

The authors would like to thank Mr. Orhan Kizilkaya and Mr. Hasan Murat Sert for their technical supports during this study and also would like to thank Prof. Dr. Mustafa Kemal Apalak for serving opportunities of Erciyes University, College of Aviation.

## References

- [1] Austin, R. 2010. Unmanned aircraft systems. Wiley.
- [2] Dink, Y., Liu, Y. C., and Hsiao, F. B. The application of extended Kalman filtering to autonomous formation flight of small UAV system. *Aircraft Engineering and Aerospace Technology*. 1(2), 154-186.
- [3] Drak, A., Hejase, M., ElShorbagy, M., Wahyudie, A., & Noura, H. 2014. Autonomous Formation Flight Algorithm and Platform for Quadrotor UAVs. *International Journal of Robotics and Mechatronics*. 1(4), 124-132.
- [4] Luca De Filippis, Giorgio Guglieri, Fulvia B. Quagliotti. 2014. A novel approach for trajectory tracking of UAVs. *Aircraft Engineering and Aerospace Technology: An International Journal*. 86 (3), 198 – 206.
- [5] Hadi, G., Varianto, R., Trilaksono, B., and Budiyo, A. 2014. Autonomous UAV System Development for Payload Dropping Mission. *Journal of Instrumentation, Automation and Systems*. 1(2), 72-77.
- [6] Grigoriadis, K. M., Carpenter, M. J. Zhu, G., and Skelton, R. E. 1993. Optimal Redesign of Linear Systems. paper presented at Proceedings of the American Control Conference, San Francisco, CA.
- [7] Grigoriadis, K. M., Zhu, G., and Skelton, R. E. 1996. Optimal Redesign of Linear Systems. *Journal of Dynamic Systems, Measurement and Control*. 118 (3), 598–605.
- [8] Krog, L., Tucker, A., Kemp, M., and Boyd, R. 2004. Topology Optimization of Aircraft Wing Box Ribs. Paper presented at 10th AIAA/ISSMO Multidisciplinary Analysis and Optimization Conference. Albany, New York, USA.
- [9] Park, K., Han, J. W., Lim, H. J., Kim, B. S. and Lee, J. 2008. Optimal Design of Airfoil with High Aspect Ratio in Unmanned Aerial Vehicles. *World Academy of Science, Engineering and Technology*, 2 (4), 171-177.
- [10] Qun, W. and Hong-quang, J. 2011. Optimal design of UAV's pod shape. Paper presented at International Symposium on Photoelectronic Detection and Imaging: Advances in Infrared Imaging and Applications Beijing, China.

- [11]Chao, H., Cao, Y., and Chen, Y. Q. 2007. Autopilots for Small Fixed-Wing Unmanned Aerial Vehicles: A Survey. Paper presented at IEEE International Conference on Mechatronics and Automation, Harbin, China.
- [12]Jung, D., Ratti, J., Tsiotras, P. 2009. Real-time implementation and validation of a new hierarchical path planning scheme of UAVs via hardware-in-the-loop simulation. *Journal of Intelligent and Robotic Systems*, 54 (1-3), 163-281.
- [13]Sartori, D. 2014. Design, implementation and testing of advanced control laws for fixed-wing UAVs. PhD dissertation, Politecnico di Torino, Torino, Italy.
- [14]Nelson, R. C. 2007. Flight Stability and Automatic Control. 2nd ed., McGraw-Hill, New York, chapters 2-6.
- [15]Zagi-The original R/C EPP foam wing homepage (2015), <http://www.zagi.com>.
- [16]Vural, S. Y. and Hajiyev, C. 2008. Autopilot system design for a small unmanned aerial vehicle. MS thesis, Istanbul Technical University, Istanbul, Turkey.
- [17]Vural, S. Y. and Hajiyev, C. 2013. LQR controller with Kalman estimator applied to UAV longitudinal dynamics. *Scientific Research Journal*. 4, 36-41.
- [18]Cardenas, E. M., Boschetti, P. J., and Celi, M. R. 2012. Design of control systems to hold altitude and heading in severe atmospheric disturbances for an unmanned airplane. Paper presented at 50th AIAA Aerospace Sciences Meeting including the New Horizons Forum and Aerospace Exposition, Nashville, Tennessee.
- [19]Jeni, S. D. and Budiyo, A. 2006. Automatic Flight Control System”, Lecture notes for Malaysian Institute of Aviation Technology.
- [20]U.S. Military Handbook MIL-HDBK-1797, 1997.
- [21]Jang, J. S., Liccardo, D. 2006. Automation of small UAVs using a low cost mems sensor and embedded computing platform.
- [22]Sultan, C. 2010. Proportional damping approximation using the energy gain and simultaneous perturbation stochastic approximation. *Mechanical Systems and Signal Processing*. 24, 2210-2224.
- [23]Oktay, T. 2012. Constrained control of complex helicopter models. PhD Dissertation, Virginia Tech.
- [24]Oktay, T. and Sultan, C. (2013), “Simultaneous helicopter and control-system design,” *Journal of Aircraft*, Vol. 50, No. 3, pp. 32-47.
- [25]Sadegh, P. and Spall, J. C. (1998), “Optimal random perturbations for multivariable stochastic approximation using a simultaneous perturbation gradient approximation”, *IEEE Transactions on Automatic Control*, 43(10), pp. 1480-1484.
- [26]He, Y. and Fu, M. C. (2003), “Convergence of simultaneous perturbation stochastic approximation for non-differentiable optimization”, *IEEE Transactions on Aerospace and Electronic Systems*, 48 (8), 1459-1463.